J|A|C|S ARTICLES

Published on Web 11/16/2010

Hysteretic Spin and Charge Delocalization in a Phenalenyl-Based Molecular Conductor

Sushanta K. Pal, Pradip Bag, Arindam Sarkar, Xiaoliu Chi,† Mikhail E. Itkis, Fook S. Tham, Bruno Donnadieu, and Robert C. Haddon*

Departments of Chemistry and Chemical and Environmental Engineering, University of California, Riverside, California 92521-0403, United States

Received August 11, 2010; E-mail: haddon@ucr.edu

Abstract: We have investigated the solid-state electronic structure and properties of a phenalenyl-based butyl-substituted neutral radical, **3**, that shows a hysteretic phase transition just above room temperature. We quantitatively analyzed the electron density distribution of this radical throughout both branches of the hysteretic phase transition using solid-state X-ray structures and found two distinct electronic states in the hysteresis loop that accompanies the phase transition. The bistability of the two electronic states was observed through a number of measurements, including IR transmittance spectra of single crystals in the vicinity of the phase transition. By comparing the changes in the crystal structures of **3** and the related ethyl-substituted radical **1** (which exhibits no hysteresis) at various temperatures, we show that the change in the interplanar $\pi-\pi$ distance within dimers is the most important structural parameter in determining the physical properties of the radicals. The large change in the C−H$\cdots\pi$ interaction in **3** occurs in concert with the spin redistribution during the phase transition, but these factors are not responsible for the hysteresis effect. We suggest that the presence of a high-temperature state inside the hysteretic loop during the cooling cycle is due to thermodynamic stability, while the existence of the low-temperature state during the heating cycle is due to the presence of a large energy barrier between the two states (estimated to be greater than 100 kJ/mol) that results from the large-amplitude motion of the phenalenyl rings and the associated lattice reorganization energy that is required at the phase transition.

Introduction

Phenalenyl (PLY) is an odd-alternant hydrocarbon with high symmetry (D_{3h}) that has the ability to form three redox species: cation, radical, and anion;[1,2] these characteristics have been exploited to produce a series of compounds having an unusual electronic structure.[3−8] In the solid state, a number of the radicals exhibit phase transitions that show clearly identifiable changes in the physical properties, including structure, magnetism, conductivity, color, and IR transmittance.[3,9−11]

We recently developed a structurally based bond order−bond length analysis that allows a quantitative determination of the location of the spin and charge density in spirobiphenalenyl neutral radical conductors such as **1**−**10** (Scheme 1), and we were able to show that the degree of spin delocalization in these compounds is intimately related to the conductivity and magnetism.[12] While the analysis does not include the effects of dispersion,[13] we presume that it is successful because the dispersion forces remain relatively constant while the changes in the electronic structure and physical properties are mainly governed by the redistribution of the spin and charge in the radicals. The analysis allowed us to rationalize some hitherto unexplained features of these compounds in terms of the

Scheme 1

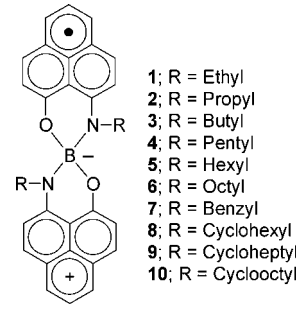

1; R = Ethyl
2; R = Propyl
3; R = Butyl
4; R = Pentyl
5; R = Hexyl
6; R = Octyl
7; R = Benzyl
8; R = Cyclohexyl
9; R = Cycloheptyl
10; R = Cyclooctyl

† Present address: Department of Chemistry, Texas A&M University-Kingsville, Kingsville, TX 78363.

(1) Reid, D. H. *Q. Rev., Chem. Soc.* **1965**, *19*, 274–302.
(2) Hicks, R. G. *Org. Biomol. Chem.* **2007**, *5*, 1321–1338.
(3) Morita, Y.; et al. *Nat. Mater.* **2008**, *7*, 48–51.
(4) Shimizu, A.; Uruichi, M.; Yakushi, K.; Matsuzaki, H.; Okamoto, H.; Nakano, M.; Hirao, Y.; Matsumoto, K.; Kurata, H.; Kubo, T. *Angew. Chem., Int. Ed.* **2009**, *48*, 5482–5486.
(5) Huang, J.; Kertesz, M. *J. Am. Chem. Soc.* **2003**, *125*, 13334–13335.
(6) Huang, J.; Kertesz, M. *J. Am. Chem. Soc.* **2006**, *128*, 1418–1419.
(7) Small, D.; Zaitsev, V.; Jung, Y.; Rosokha, S. V.; Head-Gordon, M.; Kochi, J. K. *J. Am. Chem. Soc.* **2004**, *126*, 13850–13858.
(8) Kubo, T.; Shimizu, A.; Sakamoto, M.; Uruichi, M.; Yakushi, K.; Nakano, M.; Shiomi, D.; Sato, K.; Takui, T.; Morita, Y.; Nakasuji, K. *Angew. Chem., Int. Ed.* **2005**, *44*, 6564–6568.
(9) Chi, X.; Itkis, M. E.; Kirschbaum, K.; Pinkerton, A. A.; Oakley, R. T.; Cordes, A. W.; Haddon, R. C. *J. Am. Chem. Soc.* **2001**, *123*, 4041–4048.
(10) Itkis, M. E.; Chi, X.; Cordes, A. W.; Haddon, R. C. *Science* **2002**, *296*, 1443–1445.
(11) Miller, J. S. *Angew. Chem., Int. Ed.* **2003**, *42*, 27–29.
(12) Haddon, R. C.; Sarkar, A.; Pal, S. K.; Chi, X.; Itkis, M. E.; Tham, F. S. *J. Am. Chem. Soc.* **2008**, *130*, 13683–13690.
(13) Mota, F.; Miller, J. S.; Novoa, J. J. *J. Am. Chem. Soc.* **2009**, *131*, 7699–7707.

10.1021/ja107201d

(de)localization of the spin and charge in these molecules and to show that the enhanced conductivity of the ethyl-substituted radical **1** at the magnetic phase transition is due to the generation of a complex but delocalized electronic structure and not to the formation of a diamagnetic π-dimer.[12] The structurally related butyl-substituted radical **3** is known to show similar behavior but at much higher temperatures. Furthermore, measurements of the magnetism, conductivity, and specific heat have shown that the phase transition in this compound exhibits bistability with a hysteretic width of about 25 K.[9,10,14] The phenomenon of hysteresis has attracted much attention in recent years, and many theoretical models and case-by-case mechanisms have been proposed to account for the bistability at the phase transitions.[15−25] Radicals **1** and **3** provide an excellent opportunity to study the occurrence of hysteresis because of the fact that although they share many similarities in structure, spin, and conductivity, one shows hysteresis while the other displays a smooth transition between the low- and high-temperature states. In this paper, we compare the structural changes in radicals **1** and **3** at various temperatures, particularly in the vicinity of the phase transitions, and with the help of the empirical electron densities and optical measurements, we propose a mechanism of hysteresis that may be useful in designing and understanding materials that show the hysteresis effect.

Result and Discussion

We determined the single-crystal X-ray structure of compound **3** at 10 temperatures while heating from 100 to 360 K and three additional temperatures while cooling, which allowed us to follow the evolution of the structure and the electron density distribution through the phase transition (see the Supporting Information).[12] Throughout this temperature range, compound **3** maintained the monoclinic space group $P2_1/c$ and a unit cell containing four molecules. In previous papers, we showed that the building blocks of both radicals **1** and **3** in the solid state are π-dimers[9,10] and that the active carbons in the PLY units involved in the $\pi-\pi$ interaction are superimposed (Figure 1).

When **1** and **3** are heated, both compounds undergo phase transitions in which they evolve from diamagnetic to paramagnetic π-dimers, and there is a change in the mean planar separation between the two superimposed PLYs at the phase transition, as shown in Table 1 for **3**.

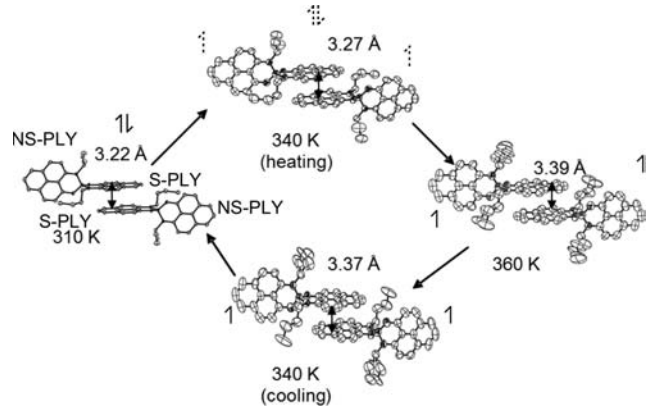

Figure 1. ORTEP views of **3** at temperatures of 310 K, 340 K (heating), 340 K (cooling), and 360 K, showing superimposed PLY (S-PLY) and nonsuperimposed PLY (NS-PLY) within the dimer of butyl-substituted radical **3** (ethyl-substituted radical **1** forms similar π-dimers). The structures show the displacement and disorder of the butyl group due to the phase transition together with the interplanar separations and limiting spin and electron density distributions of **3** as a function of temperature; the center structures refer to the two branches of the hysteresis loop. H atoms have been omitted for clarity.

We previously explained the properties and mean plane separation data for radical **3** in terms of two types of structures, even though the space group is maintained throughout the whole temperature range: (1) a low-temperature (LT) structure (or state) with mean plane separation less than the van der Waals distance (3.4 Å) and (2) a high-temperature (HT) structure (or state) with a slightly larger mean plane separation.[9,10,12] The interconversion between the two structures during heating and cooling cycles is depicted in Figure 1, where hysteresis is demonstrated by the existence of two different structures at a common temperature (center). The same two structures are also seen in radical **1**, but their interconversion does not exhibit a hysteresis effect.[9,12]

Following the previously reported method,[12] we calculated the electron density distribution among the superimposed PLYs (S-PLYs) and nonsuperimposed PLYs (NS-PLYs) as a function of temperature for butyl-substituted radical **3** (Table 1), and these data are plotted in Figure 2 as a function of interplanar separation (D) for both radicals. It is clear that neither radical exists in two discrete states (LT and HT) insofar as the electronic and solid-state structures are concerned, and the electronic configurations and interplanar separations span a surprisingly large range of values. The interplanar separations are D(**1**, LT) = 3.15−3.22 Å, D(**1**, HT) = 3.28−3.34 Å, D(**3**, LT) = 3.11−3.27 Å, and D(**3**, HT) = 3.37−3.38 Å, whereas the electronic configurations [given in terms of electron density (ED)] are the following: (**1**, LT) S-PLY, ED = 0.71−0.42e; NS-PLY, ED = 0.29−0.58e; (**1**, HT) S-PLY, 0.17−0.0e; NS-PLY, 0.83−1.0e; (**3**, LT) S-PLY, 0.95−0.48e; NS-PLY, 0.05−0.52e; and (**3**, HT) S-PLY, 0.0e; NS-PLY, 1.0e.[12] Hence, only the HT state of **3** exists in a single electronic configuration, and it is apparent that the delocalization of the electron density and the interplanar separation are strong functions of temperature. Thus, in general the LT and HT forms cannot be uniquely identified with a particular interplanar separation or electronic configuration.

In **3**, there are only two electron density distributions in the vicinity of the phase transition: (1) the LT state, where the electron is equally distributed between the two PLY units (0.5e on S-PLY and 0.5e on NS-PLY), which is accessed during the heating cycle; and (2) an HT state in which the electron is

(14) Jorge, G. A.; Kim, K. H.; Jaime, M.; Chi, X.; Hellman, F.; Itkis, M. E.; Mandal, S. K.; Haddon, R. C. *AIP Conf. Proc.* **2006**, *850*, 1315–1316.
(15) Bolvin, H.; Kahn, O. *Chem. Phys.* **1995**, *192*, 295–305.
(16) Kahn, O.; Jonas, K.; Jay, C. *Adv. Mater.* **1992**, *4*, 718–728.
(17) Kahn, O.; Martinez, C. J. *Science* **1998**, *279*, 44–48.
(18) Tchougreef, A. L. *Chem. Phys. Lett.* **1993**, *214*, 627–630.
(19) Willett, R. D.; Gomez-Garcia, C. J.; Ramakrishna, B. L.; Twamley, B. *Polyhedron* **2005**, *24*, 2232–2237.
(20) Barclay, T. M.; Cordes, A. W.; George, N. A.; Haddon, R. C.; Itkis, M. E.; Mashuta, M. S.; Oakley, R. T.; Palstra, T. T. M.; Patenaude, G. W.; Reed, R. W.; Richardson, J. F.; Zhang, H. *J. Am. Chem. Soc.* **1998**, *120*, 352–360.
(21) Brusso, J. L.; Clements, O. P.; Haddon, R. C.; Itkis, M. E.; Leitch, A. A.; Oakley, R. T.; Reed, R. W.; Richardson, J. F. *J. Am. Chem. Soc.* **2004**, *126*, 8256–8265.
(22) Brusso, J. L.; Clements, O. P.; Haddon, R. C.; Itkis, M. E.; Leitch, A. A.; Oakley, R. T.; Reed, R. W.; Richardson, J. F. *J. Am. Chem. Soc.* **2004**, *126*, 14692–14693.
(23) Fujita, W.; Awaga, K. *Science* **1999**, *286*, 261–262.
(24) Fujita, W.; Awaga, K.; Matsuzaki, H.; Okamoto, H. *Phys. Rev. B* **2002**, *65*, 64434.
(25) McManus, G. D.; Rawson, J. M.; Feeder, N.; van Duijin, J.; McInnes, E. J. L.; Novoa, J. J.; Burriel, R.; Palacio, F.; Oliete, P. *J. Mater. Chem.* **2001**, *11*, 1992–2003.

Table 1. Regression Analysis of the Change in Bond Length against the Change in Bond Order of Phenalenyl (PLY) Units in Radical **3** Using a Zero-Intercept Fit of the Form $y = a_f x$ (ref 12)

T (K)	PLY environment	R^a	slope (SD)^b	sum of slopes	electron distribution^c	D (Å)^d
100	superimposed	−0.93	−0.35 (0.04)	−0.37	0.95	3.11
	nonsuperimposed	−0.13	−0.02 (0.03)		0.05	
200	superimposed	−0.92	−0.31 (0.03)	−0.33	0.94	3.12
	nonsuperimposed	−0.48	−0.02 (0.02)		0.06	
250	superimposed	−0.89	−0.29 (0.04)	−0.33	0.88	3.16
	nonsuperimposed	−0.49	−0.04 (0.02)		0.12	
293	superimposed	−0.92	−0.28 (0.03)	−0.37	0.76	3.19
	nonsuperimposed	−0.71	−0.09 (0.02)		0.24	
310	superimposed	−0.90	−0.25 (0.03)	−0.42	0.60	3.22
	nonsuperimposed	−0.86	−0.17 (0.03)		0.40	
320+^{e}	superimposed	−0.93	−0.25 (0.03)	−0.44	0.57	3.24
	nonsuperimposed	−0.88	−0.19 (0.03)		0.43	
320−^{f}	superimposed	−0.94	−0.25 (0.03)	−0.44	0.57	3.23
	nonsuperimposed	−0.86	−0.19 (0.03)		0.43	
330+^{e}	superimposed	−0.89	−0.22 (0.03)	−0.46	0.48	3.25
	nonsuperimposed	−0.87	−0.24 (0.04)		0.52	
330−^{f}	superimposed	+0.41	0.12 (0.06)	−0.44	0	3.37
	nonsuperimposed	−0.84	−0.44 (0.07)		1	
340+^{e}	superimposed	−0.92	−0.22 (0.03)	−0.44	0.50	3.27
	nonsuperimposed	−0.84	−0.22 (0.04)		0.50	
340−^{f}	superimposed	+0.32	0.08 (0.05)	−0.35	0	3.37
	nonsuperimposed	−0.88	−0.35 (0.05)		1	
350	superimposed	0.12	0.05 (0.05)	−0.52	0	3.37
	nonsuperimposed	−0.88	−0.52 (0.08)		1	
360	superimposed	0.13	0.04 (0.05)	−0.56	0	3.38
	nonsuperimposed	−0.91	−0.56 (0.07)		1	

[a] Correlation coefficient. [b] Slopes (a_f) obtained from plots of Δr_{kl} (change in bond length) against p^f_{kl}(bond order of the frontier molecular orbital), as discussed in ref 12. Standard deviations are given in parentheses. It should be noted that positive slopes, which are not physically meaningful, have been replaced by zero where they occur. [c] Electron distribution among the frontier molecular orbitals, as determined by the ratio of the slope to the sum of the slopes. [d] Mean plane separation of the superimposed π-dimer PLY units. [e] Data collected during the heating cycle. [f] Data collected during the cooling cycle.

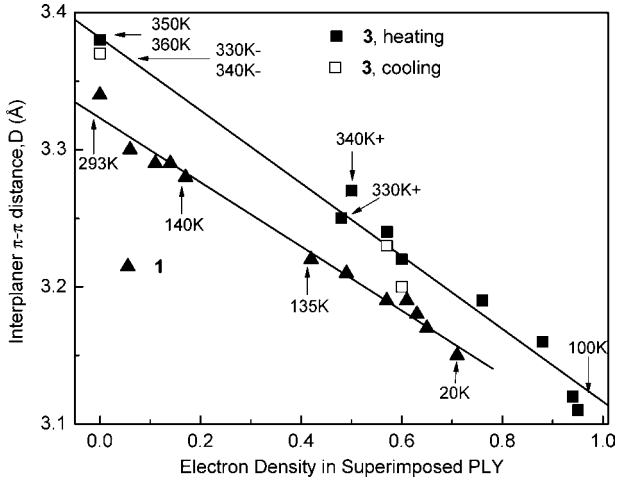

Figure 2. Plots of interplanar $\pi-\pi$ distance D vs electron density in the superimposed PLY unit for radical **1** at 20, 90, 100, 110, 120, 130, 135, 140, 150, and 293 K (▲), radical **3** in the heating cycle at 100, 200, 250, 293, 310, 320, 330, 340, 350, and 360 K (■), and radical **3** in the cooling cycle at 340, 330, 320, and 293 K (□).

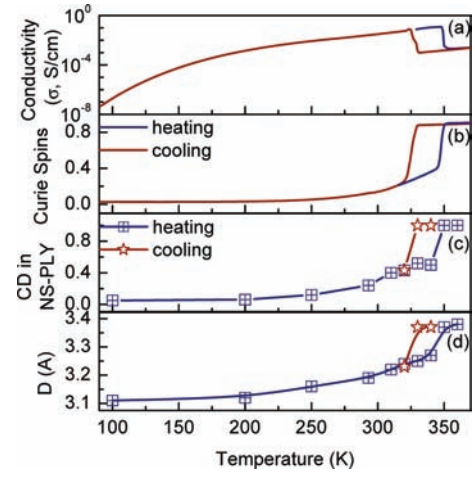

Figure 3. Physical measurements and analysis of crystals of butyl-substituted radical **3** as a function of temperature: (a) single-crystal conductivity (σ); (b) fraction of Curie spins ($n = 8\chi_p T/3$, calculated from the measured paramagnetism); (c) charge density (CD) in NS-PLY; and (d) mean interplanar separation between superimposed PLY rings (D).

completely localized (0e on S-PLY and 1.0e on NS-PLY), which is accessed during the cooling cycle. The change in the electron distribution between the two states is illustrated in Figure 1.

The physical properties of **3** as a function of temperature are shown in Figure 3,[9,10] together with the new results. As radical **3** is heated from 100 K, the charge density in the NS-PLY ring shows a gradual increase until it reaches the point where the spin (Figure 3b) and charge (Figure 3c) are equally distributed between the two rings (ED = 0.5e in both PLY rings) and the π-dimer is bound by a single electron.[7,26] Beyond this point, the charge density increases dramatically at 350 K, resulting in full charge transfer to the NS-PLY ring (ED = 1e). When **3** is cooled from 360 K, the charge density in the NS-PLY ring remains unchanged (ED = 1e) until 330 K, but below this temperature there is a sharp decrease in charge density at 320 K to the delocalized electronic structure, which is observed in all of the low-temperature structures.

(26) Lu, J.; Rosokha, S. V.; Kochi, J. K. *J. Am. Chem. Soc.* **2003**, *125*, 12161–12171.

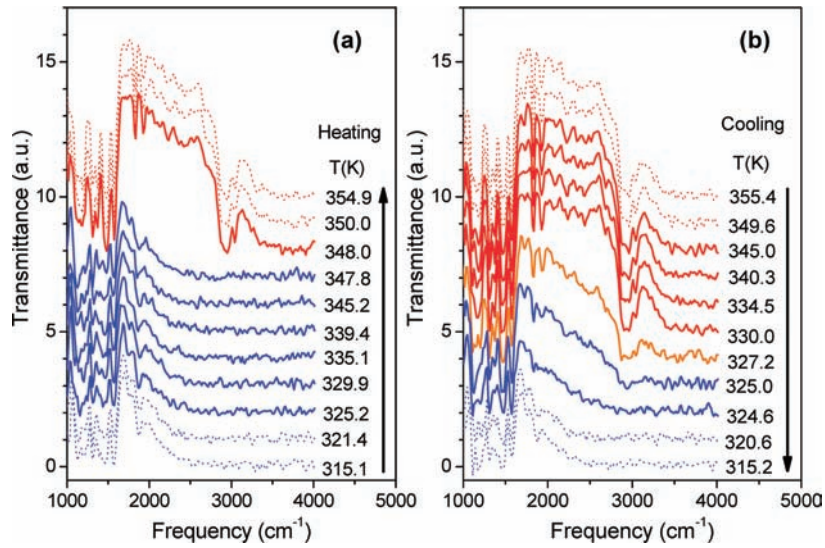

Figure 4. Hysteretic modification of the IR transmission of a single crystal of butyl-substituted radical **3** during the phase transition: (a) heating cycle; (b) cooling cycle. Red- and blue-colored spectral curves correspond to the HT and LT states of the hysteresis loop, respectively, and the spectra outside the hysteresis loop are shown with dotted lines. The transmittance spectra have been shifted vertically for clarity. Spectra at 350 K were taken from ref 10.

The Curie spin count obtained from the magnetic susceptibility data (data taken from ref 9) follows the electron density distribution obtained from the structural analysis at low temperatures, and it is clear that in this regime all of the spins localized on the NS-PLY units contribute to the susceptibility (Figure 3b). At higher temperatures, in the range 250−340 K, the system starts to become delocalized and the Curie spin count falls below the calculated charge (and spin) density in the nonsuperimposed PLY units, as would be expected from the development of closed-shell character in the wave function.[7,27−30] The π-dimer structure is maintained to the point where there is a total of just one electron binding the two S-PLY units, and this configuration maximizes the conductivity (Figure 3a; data taken from ref 9). Below this electron count, however, the PLY units separate abruptly; solution-phase data were used to demonstrate the occurrence of isolectronic PLY dimers.[7,26] In the high-temperature phase, the spins fully migrate to the NS-PLY units, leading to the recovery of the full paramagnetism of this open-shell state and a conductivity decrease of two orders of magnitude. It is clear that during the cooling cycle, the paramagnetic state is unable to readily reform the delocalized wave function, which is necessary for regeneration of the π-dimer.

The existence of two metastable states, or bistability, is also seen in the optical spectral depicted in Figure 4, from which two electronic structures can be inferred: (1) a high-temperature optically transparent structure with low conductivity (paramagnetic with the unpaired electron on NS-PLY) and (2) a low-temperature optically opaque structure with high conductivity (diamagnetic with the unpaired electron on S-PLY).[9,10,31]

In order to delineate the origin of the hysteresis found in the butyl-substituted radical **3** but not in the ethyl analogue **1**, we investigated the details of their crystal structures. It is clear from previous discussion that the strongest intermolecular interaction arises from the $\pi-\pi$ overlap within the dimers. Between π-dimers, there exist weak C−H$\cdots\pi$ interactions[32−35] formed by the aromatic C−H of one dimer and the aromatic PLY ring of a neighboring dimer (see Figure 7). The C−H bonds (blue) of an NS-PLY point toward the middle of the 13-membered S-PLY ring (NS) of a neighboring π-dimer (Figure 5), which means that the reduction in electron density in the S-PLY ring is associated with weakening of the C−H$\cdots\pi$ interaction. Figure 5b lists values of the C−H$\cdots\pi$ distance *d* between dimers and the interplanar distance *D* within dimers for both **1** and **3** at temperatures in the vicinity of the corresponding phase transitions (also see Figure 6). The interplanar distance *D* undergoes a sudden change at the phase transition for both radicals, with a hysteresis effect in the case of **3**. However, only **3** undergoes a discontinuous and large change in the C−H$\cdots\pi$ distance *d*, together with a hysteresis effect, whereas the change in *d* for **1** is negligible.

In Figure 6 we have plotted for both radicals the two intermolecular parameters that are most obviously affected by the phase change, namely, the C−H$\cdots\pi$ distance (Figure 6a) and the electron density in the S-PLY (Figure 6b), as functions of temperature. Before their respective phase transitions, both **1** (130 K) and **3** (330 K) follow a similar pattern in which the electron density in the superimposed PLY unit decreases smoothly with increasing temperature. The evolution of the electron density becomes completely different after the onset of the phase transitions: for the ethyl-substituted radical **1**, even though the electron density drops significantly, it does so continuously and does not reach zero in the vicinity of the phase transition. The electron density in the S-PLY in butyl-substituted radical **3**, however, drops abruptly to zero during the phase transition.

It is therefore clear that in radical **1** the electron density is a smooth function of the reaction coordinate and variations in the C−H$\cdots\pi$ distance at the phase transition are unimportant,

(27) Borden, W. T.; Iwamura, H.; Berson, J. A. *Acc. Chem. Res.* **1994**, *27*, 109–116.
(28) Jung, Y.; Head-Gordon, M. *J. Phys. Chem. A* **2003**, *107*, 7475–7481.
(29) Huang, J.; Kertesz, M. *J. Am. Chem. Soc.* **2007**, *129*, 1634–1643.
(30) Huang, J.; Kertesz, M. *J. Phys. Chem. A* **2007**, *111*, 6304–6315.
(31) Chi, X.; Tham, F. S.; Cordes, A. W.; Itkis, M. E.; Haddon, R. C. *Synth. Met.* **2003**, *133−134*, 367–372.
(32) Miyamura, K.; Mihara, A.; Fujii, T.; Gohshi, Y.; Ishii, Y. *J. Am. Chem. Soc.* **1995**, *117*, 2377–2378.
(33) Dougherty, D. A. *Science* **1996**, *271*, 163–168.
(34) Ma, J. C.; Dougherty, D. A. *Chem. Rev.* **1997**, *97*, 1303–1324.
(35) Philp, D.; Robinson, M. A. *J. Chem. Soc., Perkin Trans. 2* **1998**, 1641–1650.

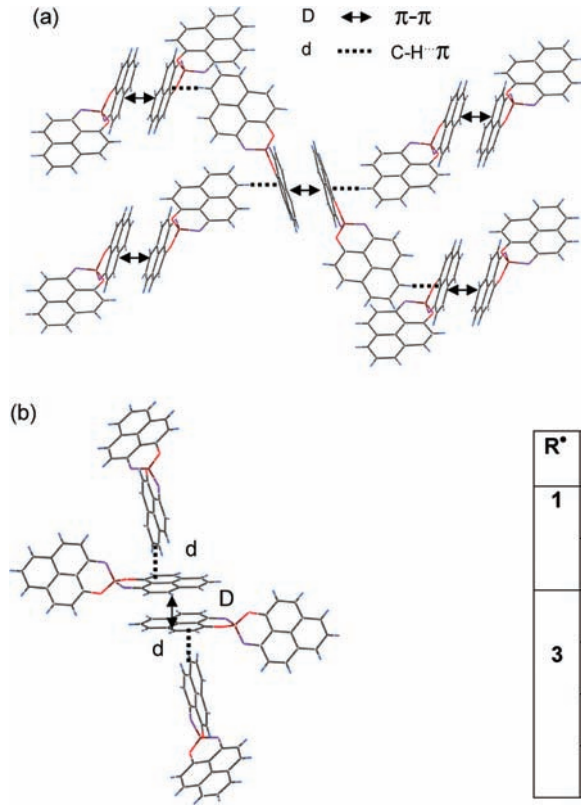

R•	T (K), State	D (Å)	d (Å)
1	100, LT	3.18	2.68
	170, HT	3.30	2.74
3	310, LT	3.22	2.89
	330, LT (h)	3.25	2.92
	330, HT (h)	3.37	3.16
	360, HT	3.39	3.17

Figure 5. (a) Packing of molecules in the crystal lattice of radical **3**, showing the $\pi-\pi$ and C−H···π interactions. (b) Interplanar distance D (Å) and the C−H···π distance d (Å) for **1** and **3** as functions of temperature (LT = low-temperature state; HT = high-temperature state; h = hysteresis loop).

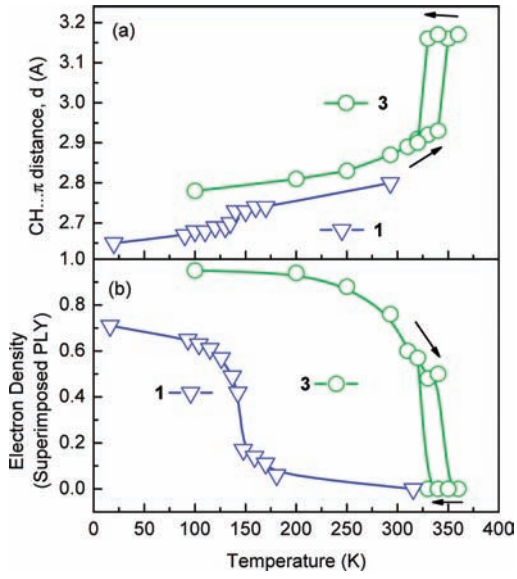

Figure 6. (a) C−H···π distance and (b) electron density in the superimposed phenalenyl (S-PLY) as functions of temperature.

whereas the abrupt change (and hysteresis) in the electron density in **3** correlates with the abrupt change (and hysteresis) in the C−H···π interaction, which undergoes a large change at the phase transition.

In order to delineate the origin of the hysteresis in butyl-substituted radical **3**, we first discuss the thermodynamic changes in ethyl-substituted radical **1** throughout the phase transition. Radical **1** exists in two limiting forms, an LT state and an HT state, that exhibit distinct interplanar separations and physical properties (Figures 2 and 6).[9,10] The thermodynamic stabilities of these two states are determined by their Gibbs free energies $G = H - TS$, where H is the enthalpy and S is the entropy. The LT state has a lower enthalpy H, while the HT state has a larger entropy S; the higher entropy of the HT state stems from the additional vibrational modes and the degrees of freedom available to the spin states of the wave function after the dissociation of the electron pairs in the covalent π-dimer bonds. Below the phase transition, enthalpy dominates, and the LT state is thermodynamically more stable. Heating decreases the free energy for both states, but the free energy of the HT state decreases faster because of its larger entropy; in the vicinity of 130 K, the free energy of the HT state becomes lower, and the phase transition occurs. The sigmoidal electron density curve for **1** (Figure 6b) can be explained by the fact that the thermal energy favors the disruption of the electron pairing while the C−H···π interaction is a constant factor favoring the presence of electron density in the superimposed rings; thus, even after the phase transition, the electron density in **1** does not fully migrate to the NS rings (in contrast to **3**).

The situation for radical **3** is similar in the LT state, which exhibits a gradual evolution of the electron density from low temperatures until 325 K, at which point the HT phase becomes thermodynamically favored, just as occurs for **1** at 130 K. However, the phase transition for butyl-substituted radical **3** includes the disruption of the C−H···π interaction and a large lattice reorganization, in contrast to the case for ethyl-substituted radical **1**. These effects contribute to the energy barrier, which is sufficiently large to maintain the LT state until 350 K, at which point both the interplanar distance and the C−H···π bond distance increase dramatically and the electron moves to the nonsuperimposed PLY ring. During the cooling process, the HT state remains thermodynamically stable until 325 K, where a

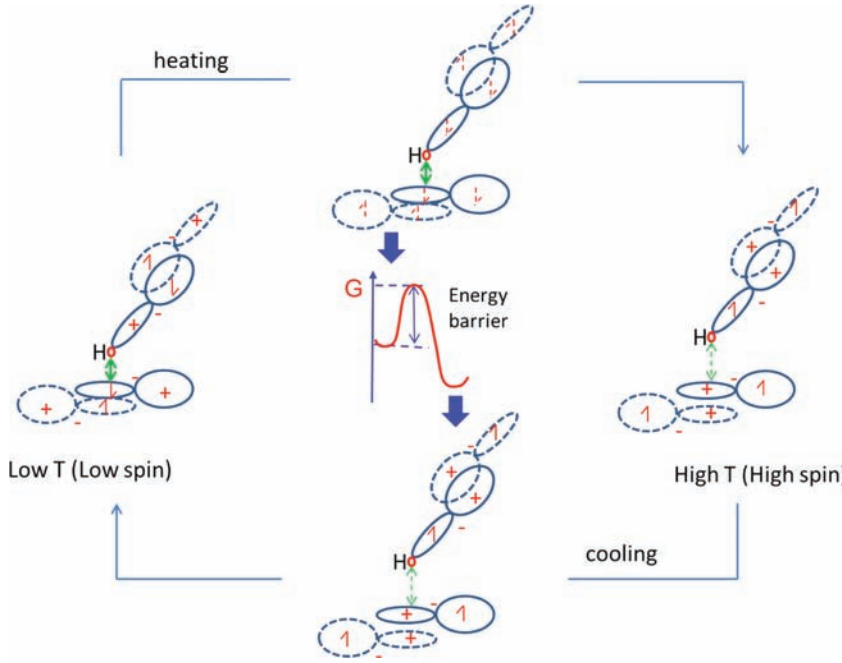

Figure 7. Schematic illustration of the C−H···π distance change during the phase transition and the energy barrier that is responsible for the hysteresis in butyl-substituted radical **3**.

reduction in the interplanar distance occurs, accompanied by the motion of the PLY rings and the reformation of the C−H···π interaction, and the electron density becomes equally distributed throughout the PLY rings. The proposed mechanism is illustrated in Figure 7, where the presence of the HT state within the hysteresis loop (during cooling) is due to its thermodynamic stability (lower free energy), while the existence of the LT structure in the hysteresis loop (heating) is due to an energy barrier that includes the lattice reorganization and the rupture of the C−H···π interaction.

We now turn to a discussion of this energy barrier and the reasons why it leads to hysteresis in butyl-substituted radical **3** but not in ethyl-substituted radical **1**. On the basis of literature estimates, it seems that the upper bound for the enthalpy associated with the C−H···π interaction is ΔE(C−H···π) < 10 kJ/mol.[32−35] The solution value for the enthalpy for π-binding of a pair of phenalenyl radicals (2PLY → PLY_2) is $\Delta H_D = -40$ kJ/mol, which may be compared with the theoretical (gas-phase estimate) $\Delta E_D = -46$ kJ/mol, whereas the analogous values for the π-binding of a phenalenyl cation and a phenalenyl radical ($PLY^+ + PLY \rightarrow PLY_2^+$) are $\Delta H_P = -27$ kJ/mol and $\Delta E_D = -84$ kJ/mol.[7,36]

The π-binding contributions to the dimerization processes of the PLYs are present in the phase transitions of both **1** and **3**, and the electron densities during the phase transitions are similar (Figure 6). Thus, these cannot be the origin of the hysteresis observed for **3**. This raises the question of the height of the energy barrier in Figure 7 that is necessary to allow the crystallographic refinement of distinct structures at a common temperature, say $T = 330$ K. If we assume that a half-life of $t_{1/2} = 10^4$ seconds is necessary for the data collection, then we can obtain a maximum unimolecular rate constant $k = (\ln 2)/t_{1/2} < 6.9 \times 10^{-5}$ s^{-1} for transits over the energy barrier between the LT and HT states. Thus, using the Arrhenius equation with a frequency factor (A) of 10^{13} s^{-1},[37] we obtain a minimum activation energy (E_a) of >100 kJ/mol for the energy barrier in Figure 7 to enable the observation of both the LT and HT states by X-ray analysis and the other measurements given in Figures 2 and 1 at $T = 330$ K. Thus, the C−H···π interaction can play only a very small role in the hysteresis, although it is clear that the electron density redistribution and the strength of the C−H···π interaction operate in concert during the hysteretic phase transition in radical **3**, and the former is the determining factor in the electronic and magnetic properties (Figure 3 and 4). It therefore seems that the energy barrier in Figure 7 originates from the energy required for the molecules to redistribute themselves in the lattice at the phase transition, which presumably may be attributed to the steric repulsion between a number of intermolecular contacts that must be surmounted along the reaction coordinate. It is clear from Figure 6 that in the case of the butyl-substituted radical, the phase change is associated with a large displacement of the molecules in the lattice and also with disorder in the butyl groups; these crystallographic rearrangements are reflected in the large change in the unit cell volume of **3** within the hysteresis loop (Figure 8).

Conclusion

In summary, careful examination of the crystal structures at various temperatures has allowed us to identify the degree of spin and charge density (de)localization in butyl-substituted radical **3** throughout the phase transition, and this has enabled us to understand some of the unexplained features of the electronic structure and physical properties of this radical. The analysis has shown that the enhanced conductivity of **3** at the magnetic phase transition is due to a delocalized electronic structure rather than to the formation of the diamagnetic

(36) Small, D.; Rosokha, S. V.; Kochi, J. K.; Head-Gordon, M. *J. Phys. Chem. A* **2005**, *109*, 11261–11267.

(37) Benesi, A.; Bertermann, R.; Forster, H.; Heubes, M.; Jackman, L. M.; Koritsanszky, T.; Luger, P.; Mayer, A.; Quest, H.; Maximilian, S.; Zobel, D. *J. Am. Chem. Soc.* **2000**, *122*, 4455–4463.

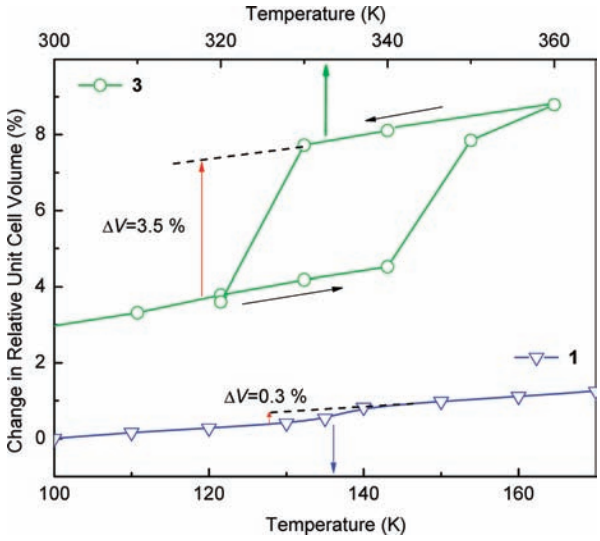

Figure 8. Changes in relative unit cell volumes for **1** (top axis) and **3** (bottom axis) with temperature.

π-dimer. Furthermore, we have shown that in addition to the strong $\pi-\pi$ interactions within dimers, there are weak C−H···π interactions between dimers that are strongly affected by the hysteresis; while the C−H···π distance changes dramatically at the phase transition in butyl-substituted radical **3**, there is little variation of this distance in ethyl-substituted radical **1**. We suggested that the electron density distribution is correlated with the strength of the C−H···π interaction in **3**; however, while these two parameters are strongly affected by the phase transition, we have shown that they are not responsible for the occurrence of hysteresis in **3**, although the physical properties are determined by the strength of the $\pi-\pi$ interaction. We propose that the presence of a high-temperature state inside the hysteresis loop during cooling is due to its thermodynamic stability, while the presence of a low-temperature state inside the loop during heating is due to the presence of an energy barrier that separates the low- and high-temperature states (Figure 7). We estimated this energy barrier to be greater than 100 kJ/mol, which is far too large to be solely attributed to the rupture of the C−H···π interaction, so the presence of the energy barrier and the occurrence of hysteresis in **3** is best explained by the large-amplitude motion of the phenalenyl rings and the associated lattice reorganization energy that is required at the phase transition.

Experimental and Calculation Section

Preparation of Radical 3. Bis(9-*N*-butylamino-1-oxophenalene)boron (**3**) was prepared and crystallized according to a literature procedure.[9]

X-ray Crystallography. A black needle fragment (0.47 × 0.19 × 0.13 mm^3) of **3** was used for the single-crystal X-ray diffraction study. The crystal was mounted on a glass fiber with epoxy resin. X-ray intensity data were collected at 100(2), 200(2), 250(2), 293(2), 310(2), 320(2), 330(2), 340(2), 350(2), and 360(2) K in the heating cycle and at 340(2), 330(2), and 320(2) K in the cooling cycle on a Bruker APEX2 (version 2.0−22) platform-CCD X-ray diffractometer system (Mo radiation, λ = 0.71073 Å, 50 kV/40 mA power).[38] Absorption corrections were applied to the raw intensity data using the SADABS program.[39] The Bruker SHELXTL software package (version 6.14) was used for phase determination and structure refinement.[40] Atomic coordinates and isotropic and anisotropic displacement parameters for all of the non-hydrogen atoms were refined by means of a full-matrix least-squares procedure on F^2. All of the H atoms were included in the refinement at calculated positions riding on the atoms to which they were attached.

Single-Crystal IR and UV−Vis Transmission Spectroscopy. For the IR transmission measurements, a rectangular slit with dimensions of 60 × 700 μm^2 was formed on a KRS-5 substrate by thermal evaporation of a 200 nm copper film using a shadow mask. A single crystal of **3** with dimensions of 35 × 100 × 950 μm^3 was placed on the substrate so that the opening of the slit was completely covered by the crystal. In the finished mounting, only radiation transmitted through the sample was detected. Data were normalized to the spectrum through the slit itself without the crystal. The IR transmission measurements employed a Nicolet Magna-IR 560 ESP FTIR spectrometer and variable-temperature optical cryostat.

Calculations. The calculated partial bond orders (p^f_{kl}) were taken from ref 12 and were based on standard Hückel molecular orbital parameters.[41,42] The structure of radical **3** was taken from ref 9 and that of the reference cation **3**$^+$ from ref 31.

Acknowledgment. The authors are grateful to O. P. Clements, C. M. Robertson, and Professor R. T. Oakley (University of Waterloo) for crystallographic experiments and useful discussions. This work was supported by the Office of Basic Energy Sciences, U.S. Department of Energy, under Grant DE-FG02-04ER46138.

Supporting Information Available: Illustrations of the unit cell of **3** and the overlaps in the π-dimers; plots of the change in bond length (Δr_{kl}; *y* axis) versus the differential change in bond order (p^f_{kl}; *x* axis) in the form $y = a_f x$ using bond length and Δr_{kl} values for radical **3**; plots of change in relative unit cell volume versus temperature for **1** and **3**; tables of distance data at various temperatures; complete ref 3; and crystallographic data for **3** from 100 to 360 K (CIF). This material is available free of charge via the Internet at http://pubs.acs.org.

JA107201D

(38) *APEX2 Software Reference Manual*, version 2.0−22; Bruker Analytical X-ray Systems, Inc: Madison, WI, 2004.
(39) *SADABS Software Reference Manual*, version 2004/1; Bruker Analytical X-ray Systems, Inc: Madison, WI, 2004.
(40) *SHELXTL Software Reference Manual*, version 6.14; Bruker Analytical X-ray Systems, Inc: Madison, WI, 2008.
(41) Streitwieser, A. *Molecular Orbital Theory for Organic Chemists*; Wiley: New York, 1962.
(42) Haddon, R. C. *J. Am. Chem. Soc.* **1980**, *102*, 1807–1811.